Article

Multi-Objective Optimization of Fiber Laser Cutting of Stainless-Steel Plates Using Taguchi-Based Grey Relational Analysis

Yusuf Alptekin Turkkan [1], Muhammed Aslan [2], Alper Tarkan [3], Özgür Aslan [3], Celalettin Yuce [2] and Nurettin Yavuz [2],*

[1] Department of Electronics and Automation, Bursa Uludag University, 16850 Bursa, Turkey
[2] Department of Mechanical Engineering, Bursa Uludag University, 16059 Bursa, Turkey
[3] NUKON Laser Machine Metal Industry, 16140 Bursa, Turkey
* Correspondence: nyavuz@uludag.edu.tr

Abstract: Stainless-steel has become a widely preferred material type in the marine, aerospace, sanitary, industrial equipment, and construction industries due to its superior corrosion resistance, high mechanic properties, high strength, formability, and thermal and electrical conductivity. In this study, a multi-objective optimization method based on grey relational analysis was employed to optimize the fiber laser-cutting parameters of cutting speed, focal position, frequency, and duty cycle. Surface roughness and kerf width, which are the two most important parameters that determine laser-cutting quality, were simultaneously optimized. In order to assign the optimum level of each parameter individually, the Taguchi technique was applied. The cutting surface morphology was examined according to the grey relational grade with a 3D optical profilometer, and maps of the cutting surfaces were created. According to the results achieved using Analysis of Variance (ANOVA), it was seen that the parameters that affected surface roughness and kerf width the most were duty cycle, with a contribution rate of 49.01%, and frequency, with a contribution rate of 31.2%. Frequency was the most important parameter in terms of multiple responses, with a contribution rate of 18.55%. Duty cycle and focal position were the second and third most effective parameters, respectively. It was determined that the optimum parameter values for minimum surface roughness and minimum kerf width that could be obtained with the fiber laser cutting of 20 mm thick AISI 304L (DIN EN 1.4301) material were 310 mm/min cutting speed, −11 mm focal position, 105 Hz frequency, and 60% duty cycle.

Keywords: laser cutting; stainless-steel; parameter optimization; Taguchi; grey relational analysis

1. Introduction

In line with the technological evolution in recent years, developments in laser technology have also been achieved in the industry, and laser-cutting methods have become widely used for cutting metal or non-metallic materials. Laser cutting stands out due to machining quality and cost saving, among other conventional material cutting processes. The main advantages of laser cutting are precision, automation, high speed, reproducibility, high quality, cost effectiveness, and non-contact cutting possibility [1]. Laser cutting is performed by focusing a laser beam on the cutting area of the metal surface. With the heat generated by the focused beam, evaporation occurs in the material, and a hole is formed. Afterwards, the metal is melted by moving the laser beam, and melted material is removed from the part with auxiliary gas [2]. Another important advantage is creating a narrow heat-affected zone with the beam, which can be focused on a very small area, which also minimizes material loss [3].

Nd:YAG, carbon dioxide (CO_2), and fiber lasers are commonly used for the laser-cutting process [4]. Before fiber lasers became widespread, CO_2 lasers were more advanta-

geous for cutting thick materials, while Nd:YAG lasers were used on thin materials that required precise cutting. However, with its high power, high beam quality and efficiency, operating at wavelengths of 1060–1080 μm, fiber lasers have started to be employed in the industry more than other laser types [5,6]. Thanks to their superior properties, fiber lasers allow a deeper effect to be created, long-focus lenses to be used, less damage to optical lenses to be caused, and long-distance applications to be achieved. Since the produced laser beam is transmitted with a flexible fiber optic cable without any need for a mirror in the cutting head, there is no power loss, and there is no need for an additional cooling system. The energy efficiency of fiber lasers is also quite high. The power required to cut the same thickness of steel material at a given speed is much lower in fiber lasers. A high-power fiber laser cutter is capable of cutting up to five times faster than a conventional CO_2 laser cutter and utilizes half the operating costs [7,8]. Additionally, when comparing a 2 kW fiber laser beam with a 4 kW CO_2 laser beam, the fiber laser has approximately five times greater power density. In addition, due to its shorter wavelength, fiber lasers have two times greater absorption [9]. In addition, 3 kW fiber lasers can cut 1 mm-thick stainless-steel at around 30 m/min, while a 5 kW CO_2 laser-cutting machine can only achieve one-third of that speed [10].

The quality of the laser-cutting process is defined by examining the roughness, geometry, morphology, and metallurgical properties of the cut sample. The desired level of these quality characteristics depends on the process parameters selected in accordance with the material to be cut. Studies have shown that laser power, speed, laser mode, feed rate, focal distance, auxiliary gas type, and pressure are the parameters that affect cutting quality the most [11,12]. It is vitally important to choose the optimum process parameter combination for the purpose of achieving high-quality cutting surfaces at high production rates. The main characteristics of the products after laser-cutting process, i.e., surface roughness, kerf width, hardness, and work piece removal rate, are directly related to these process parameters [13].

Stainless-steel (SS) sheets are important engineering materials used in many applications, such as defense industry, oil industry, machinery parts, automotive, chemical industry, sanitary applications, and equipment for foodstuff. Among the types of stainless-steel, the AISI 304L (DIN EN 1.4301) grade group constitutes approximately 50% of usage [14]. Despite many advantages, stainless-steel materials are not suitable for cutting with oxygen because they contain high levels of chromium in their composition. For this reason, the laser-cutting process has a very important role in the processing of such materials [15]. Many researchers have dealt with cutting parameters, which have a profound effect on the cutting surface quality of a product; research on optimization with the help of different experimental design methods has also been conducted [16–18]. Researchers used 10 mm-thick stainless-steel plates to compare the surface quality obtained with fiber lasers and CO_2 lasers. Ultimately, fiber lasers gave much better results than CO_2 lasers [19]. Fomin et al. stated that fiber lasers were more efficient than CO_2 lasers in a N_2 auxiliary gas atmosphere for cutting stainless-steel [20]. Li investigated the effect of cutting speed, focal length and laser power parameters on kerf and surface roughness using RSM (Response Surface Methodology) [21]. Li stated that the continuous increase in laser power reduces surface roughness. Further, Jadhav et al. examined the parameters that affected the surface roughness of AISI 304L (DIN EN 1.4301) stainless-steel materials and emphasized that increasing laser power and gas pressure decreased the surface roughness values. It was detected that if the laser-cutting speed increased, the surface roughness value also increased [22].

As a result of the literature search, it was determined that many researchers have carried out studies on optimizing process parameters for the laser cutting of different material types. However, most of the studies have targeted the cutting of relatively thin sheets (≤10 mm) [6,7,23,24]. When cutting thick metal, the accumulation of molten metal on the surface of the material and the accumulation of heat generated during the perforation process cause turbulence in the auxiliary airflow and excessive heat input, resulting

in excessive combustion. Additionally, thick-section metal cutting using the high-power fiber laser has been reported to produce a poorer cut quality with more complex striation patterns than are typical in CO_2 laser cutting [7]. Therefore, one of the unique aspects of the study is parameter optimization for fiber laser-cutting stainless-steel material with a thickness of 20 mm. Another novel aspect of this study is that it aims to optimize different cutting parameters (frequency, duty cycle). It has been observed that the optimized cutting parameters are generally laser power, focus position, gas pressure, and cutting speed [12,14,15,25]. It is thought that the results obtained in this respect will make an important contribution to the literature. On the other hand, to achieve ideal cutting parameters, simple objective optimizing methods are not sufficient enough, whereas opposing and different objectives have to be optimized altogether. The current study deals with developing a multi-objective optimization design in terms of grey relational analysis (GRA), which aims to optimize the process parameters in fiber laser cutting to observe surface roughness and kerf width together.

2. Experimental Procedure

2.1. Selection of Material

Fiber laser cutting is commonly used for thin-sheet metals under a thickness of 2 mm. Thicker stainless-steel materials are often cut by a Computer Numerical Control (CNC) Router in industrial applications. Thanks to the excellent advantages of fiber laser technology in order to achieve a new approach, we adopted a thick material for our study. Within the scope of this study, we applied a cutting process for a thickness of 20 mm AISI 304L (DIN EN1.4301) quality SS material on a CNC-controlled fiber laser. Mechanical and physical properties and chemical composition of AISI 304L (DIN EN 1.4301) material are presented in Table 1. The properties are received according to EN 10204 3.1 Quality Certificate from Stainless-Steel Manufacturer [26].

Table 1. Properties of Stainless-Steel AISI 304L (DIN EN 1.4301) Material.

Chemical Composition	C (%) = 0.020	Mn (%) = 1.30	Si (%) = 0.44	P (%) = 0.036
	S (%) = 0.0021	Cr (%) = 18.36	Ni (%) = 8.05	Mo (%) = 0.164
	Al (%) = 0.0038	Co (%) = 0.179	Cu (%) = 0.2591	N (ppm) = 475
Mechanical properties	Hardness 89.33 HRB	Yield Strength (0.2%) 407 MPa	Tensile Strength 674 MPa	Modulus of Elasticity 200 kN/mm^2
Physical properties	Density 7.9 g/cm^3	Specific Heat Capacity 500 J/kg K	Thermal conductivity 15 W/m K	Electrical resistivity 0.73 Ω mm^2/m

2.2. Experimental Setup

The test samples were cut out from a 20 $\times$ 1000 $\times$ 1000 mm AISI 304L (DIN EN 1.4301) plate, with the dimensions of 20 $\times$ 50 $\times$ 50 mm. A NUKON brand VENTO LINEAR 315 8000W bench (NUKON Inc., Bursa, Turkey) with maximum acceleration of 30 m/s^2 was used as a laser-cutting bench. During the cutting, a 200 mm focus lens, a Ø5 mm nozzle, and a continuous mode (CW) laser beam were used. In all experiments, N_2 gas was used with a constant pressure of 12 bar as an auxiliary gas. As a result of the preliminary trials, cutting process parameter levels were determined, as were the ranges of the parameters selected (Table 2).

After cutting, the arithmetic average of roughness profile (Ra) values was recorded on the cut surfaces of the samples with a Mitutoyo SJ-301 measuring device (Mitutoyo, Kanagawa, Japan). The Ra value was received by y-coordinates arithmetic average absolute values corresponding to the surface roughness profile. Ra also defines the arithmetic average deviation of the y-coordinates of the surface roughness from the centerline. The kerf widths on the upper surfaces of the cut pieces were measured with Mitutoyo PJ-A3005D-50 (Mitutoyo, Kanagawa, Japan) model profile projector device. Measurements

were taken from three different points, which were determined at equal intervals, on each sample. The average of these three measurements was recorded as the kerf width of that sample. This process was repeated for each sample. In order to examine the cutting surface morphologies depending on the laser parameters, 3D topological maps of the cutting surfaces were created by using an optical profilometer (Phase View, Le Buisson, France).

Table 2. Fiber laser-cutting-process parameters and their levels.

Parameters	Units	Symbols	Level I	Level II	Level III	Level IV
Cutting Speed	mm/min	CS	250	270	290	310
Focal Position	mm	FP	−11	−12	−13	−14
Frequency	Hz	F	45	65	85	105
Duty Cycle	%	DC	50	60	70	80

2.3. Grey Relational Analysis with the Taguchi Method

Taguchi is one of the most prevalent Design of Experiment (DOE) Analysis Methods that provides a simple and important technique for optimizing the process parameters of different numerical and experimental research [27–29]. The Taguchi method uses orthogonal arrays (OA). To properly establish the OA, the total degree of freedom (DOF) has to be defined at the beginning step. The degree of freedom (DOF) of each process parameter is achieved by subtracting one from the design variable values. In this present study, since there are four factors with four levels (speed, focal position, frequency and duty cycle), the DOF of the chosen orthogonal arrays (OA) was selected as L16, which should be higher than the total DOF (Table 3).

Table 3. Results of Experiment with Design Parameters and Responses and S/N Ratios.

Exp. No.	Parameters				Responses		S/N Ratios	
	CS (mm/min)	FP (mm)	F (Hz)	DC (%)	SR (μm)	KW (mm)	SR (μm)	KW (mm)
1	250	−11	45	50	11.20	0.38	−20.987	8.404
2	250	−12	65	60	13.55	0.33	−22.637	9.629
3	250	−13	85	70	14.53	0.15	−23.245	16.47
4	250	−14	105	80	14.09	0.30	−22.976	10.45
5	270	−11	65	70	11.78	0.35	−21.424	9.118
6	270	−12	45	80	12.97	0.33	−22.261	9.762
7	270	−13	105	50	9.80	0.33	−19.825	9.762
8	270	−14	85	60	11.15	0.38	−20.945	8.519
9	290	−11	85	80	13.16	0.33	−22.386	9.762
10	290	−12	105	70	12.82	0.42	−22.157	7.432
11	290	−13	45	60	13.26	0.35	−22.450	9.118
12	290	−14	65	50	9.13	0.48	−19.211	6.466
13	310	−11	105	60	8.31	0.33	−18.387	9.762
14	310	−12	85	50	11.22	0.32	−20.998	9.762
15	310	−13	65	80	13.82	0.45	−22.808	6.935
16	310	−14	45	70	12.79	0.38	−22.138	8.519

To establish the parameters' effects on responses, signal-to-noise ratios (S/N) were applied as sensitivity indicators of the desired features of the factors in the Taguchi method. Performance of (S/N) ratios can be evaluated in three categories: larger is better, smaller is better, and nominal is the best. In this study, surface roughness (SR) and kerf width (KW) minimization are the objective functions; moreover, the smaller S/N ratios selected were better, where y_i defines the response data from the experiment of the *i*th parameter and *n* defines the number of experiments (Equation (1)).

$$\frac{S}{N} = -10log\left[\frac{1}{n}\sum_{i=1}^{n} y_i^2\right] \tag{1}$$

Analysis of variance (ANOVA) is a statistical method that is commonly used to assign a participation ratio, as well as ordering parameters by results of the analysis. In this study, the influences of each process of variable parameters on responses (surface roughness and kerf width) are described by ANOVA. The significant value of statistical analysis is equal to a 95% safety level using this method. Not only was the Taguchi method used to define variable parameters in multi-responses, but so too was the GRA method, which was also used to efficiently define the complicated relation of multiple responses. Using this methodology, the first of all the performances of responses was changed into a comparability sequence; additionally, the grey relational coefficient (GRC) between all comparable and ideal target sequences was estimated. However, using the grey relational coefficient, the reference sequence and every comparable sequence can be received. An optimum response can be achieved if a comparability sequence is transferred to a response with the highest grey relational grade (GRG) computed between a reference sequence and a comparable sequence.

In this study, the data used in GRA were normalized. Due to the desired smaller roughness and kerf width, Equation (2) was used for normalization. In this equation, $minx_i^0(k)$ represents the minimum value of $x_i^0(k)$, $maxx_i^0(k)$ represents maximum $x_i^0(k)$, and $y_i(k)$ represents the normalized value. x^0 also represents the best optimized value.

$$y_i(k) = \frac{maxx_i^0(k) - x_i^0(k)}{maxx_i^0(k) - minx_i^0(k)} \tag{2}$$

After normalization, the grey relational coefficient (GRC) is defined with Equations (3) and (4) to discover the relation between the real and ideal sequences. The weight factor determinations for each response are crucial in the GRA method. However, the effect of surface roughness and kerf width on the quality of the cutting surface is greater than other quality characteristics. Therefore, the weights of the responses should not be chosen without a reasonable quantitative basis to increase or decrease its importance. In most of the studies, the weights of the responses are generally determined to be equal [30–35]. ξ represents the coefficient of identification as 0 ... 1, and is usually accepted as 0.5. Δmax represents the maximum and Δmin represents the minimum value of Δ_{0i}. $y_0(k)$ represents the comparable sequence and $y_i(k)$ represents the reference sequence. Δ_{0i} also states the difference between $y_0(k)$ and $y_i(k)$.

$$\gamma_i(k) = \frac{\Delta min + \xi\Delta max}{\Delta_{0i}(k) + \xi\Delta max} \tag{3}$$

$$\Delta_{0i}(k) = \|y_0(k) - y_i(k)\| \tag{4}$$

In the last step, the grey relational grade (GRG) is obtained with the help of a normalized weight factor. The grey relational grade represents the correlation level between the

comparable sequences and reference sequences. The best optimum level of cutting process parameters is defined by the highest grey relational grade.

$$GRG = \sum_{k=1}^{n} \omega_k \gamma_i(k) \tag{5}$$

ω_k indicates each response's normalized weight factor when $\sum_{k=1}^{n} \omega_k = 1$.

3. Results and Discussion

In this research, the Taguchi method was first applied to establish the effect of cutting process parameters for every response individually. Experimental data for surface roughness and kerf width were achieved by an L16 orthogonal array, which was utilized to create a combination of cutting process parameters. S/N ratios and the responses are illustrated in Table 3. The gap between max and min S/N ratios shows each factor's effect on the response; furthermore, each cutting process parameter on the responses is illustrated in Figures 1 and 2.
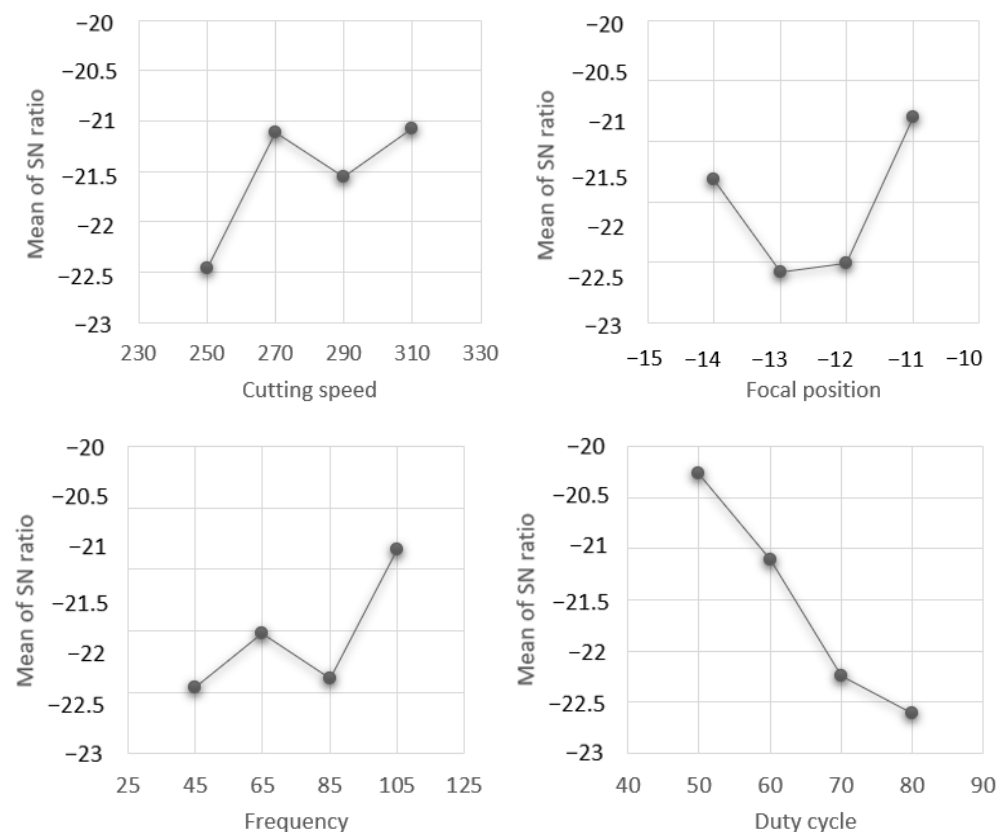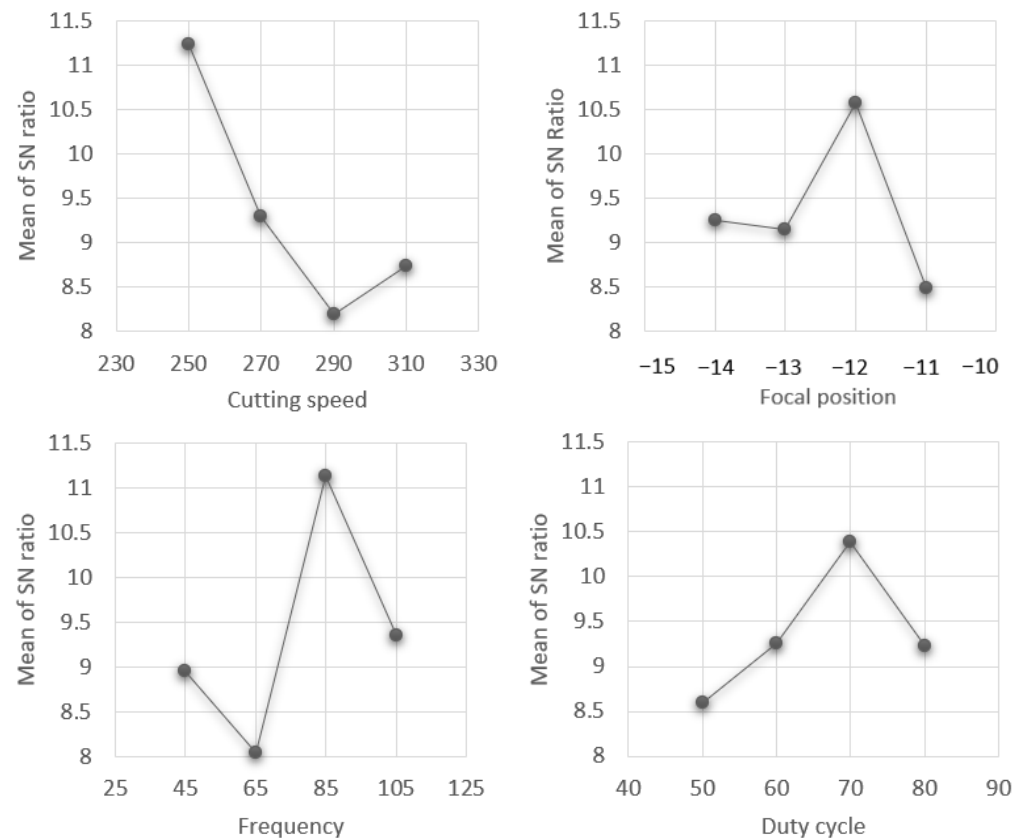

Figure 1. S/N ratios plot effects for the responses of surface roughness.

The analysis of variance (ANOVA) method was applied to discover the factor effect ratios of every cutting process parameter on kerf width and surface roughness (Table 4). As shown in the ANOVA results, DC and F were the most important process parameters on SR and KW, respectively. According to results achieved by ANOVA, the order of importance for SR is DC > CS > FP > F; for KW, it is listed as F > CS > FP > DC. According to the results achieved by ANOVA, the most effective process parameter on KW was frequency, with a ratio of 31.2%. DC was found to be the most important process parameter on SR, with a ratio of 49.01%. If the results are evaluated, it can be easily seen that inclinations achieved by ANOVA and Taguchi methods are the exact same for every response. According to the S/N ratios, the optimum process parameters for minimum surface roughness were determined as a cutting speed of 310 mm/min, a focal position of −11 mm, a frequency of

105 Hz, and a duty cycle of 50%. Additionally, the optimum process parameters for kerf width were determined as cutting a speed of 250 mm/min, a focal position of -12 mm, a frequency of 85 Hz, and a duty cycle of 70%. These results are also seen in Figures 1 and 2. Based on these results, the minimum surface roughness was obtained at the lowest duty cycle (50%), and minimum kerf width was obtained a 85 Hz frequency.

Figure 2. S/N ratios plot effects for the responses of kerf width.

Table 4. Contribution ratios and ANOVA results on surface roughness and kerf width.

	DoF	Adj SS	Adj MS	F-Value	p-Value	Contr. (%)
Surface Roughness						
CS	3	9.271	3.090	2.19	0.268	18.46
FP	3	7.705	2.568	1.82	0.317	15.34
F	3	4.396	1.465	1.04	0.488	8.75
DC	3	24.609	8.203	5.82	0.091	49.01
Error	3	4.231	1.410			8.43
Kerf Width						
	DoF	Adj SS	Adj MS	F-Value	p-Value	Contr. (%)
CS	3	0.0236	0.0078	1.24	0.432	29.1
FP	3	0.0079	0.0026	0.42	0.755	9.74
F	3	0.0253	0.0078	1.24	0.433	31.2
DC	3	0.0053	0.0017	0.28	0.838	6.54
Error	3	0.0190	0.0063			23.43

Results of the Taguchi and ANOVA analyses show that, to obtain minimum SR and minimum KW, four different process parameter combinations need to be found. However, cutting quality combines these parameters together. Thus, it is very important to use GRA to optimize surface roughness and kerf width together by simplifying this process with a single function. The GRC of surface roughness (GRC$_{SR}$) and kerf width (GRC$_{KW}$) was computed by using Equations (3) and (4), shown in Table 5.

Table 5. Grey relational analysis results.

Exp. No.	GRC$_{SR}$	GRC$_{KW}$	GRG	RANK
1	0.518	0.414	0.466	7
2	0.373	0.474	0.423	12
3	0.333	1.000	0.667	2
4	0.350	0.520	0.435	11
5	0.472	0.448	0.460	8
6	0.400	0.481	0.441	9
7	0.676	0.481	0.579	3
8	0.523	0.419	0.471	6
9	0.391	0.481	0.436	10
10	0.408	0.371	0.390	15
11	0.386	0.448	0.417	13
12	0.791	0.333	0.562	4
13	**1.000**	**0.481**	**0.742**	**1**
14	0.517	0.481	0.499	5
15	0.361	0.351	0.356	16
16	0.410	0.419	0.415	14

In this study, with the help of the detected GRG values, the response graphs were generated for each factor level. The largest GRG value was achieved by the combination of CS4, FP1, F4, and DC1, as illustrated in Figure 3. Thus, the fifth experiment (CS$_4$FP$_1$F$_4$DC$_1$) with a CS of 310 mm/min, an FP of -11 mm, an F of 105 Hz, and a DC of 50% are the optimum parameter combinations of the laser-cutting operation.

The ANOVA analyzing method was applied to calculate the participation of every parameter on multiple responses. In Table 6, the parameter of frequency (F) is the most important variable on the multiple responses, with an effect of 18.55%. The duty cycle (DC) and focal position (FP) are the second (2nd) and third (3rd) most important process parameters, respectively. Finally, we can clearly emphasize that the results achieved from ANOVA and GRG affirm each other.

According to GRG values, the cutting surface morphology was examined carefully. Additionally, the maps of surfaces obtained after cutting process were created by a 3D optical profilometer for the samples with the highest, lowest, and average GRG values to comply with their GRG values. Topological maps of surfaces obtained after the cutting process are illustrated in Figure 4. The regions where the height is zero in the images are expressed with colors in yellow tones. The positive height increases with the red color and the negative depth with the green color.
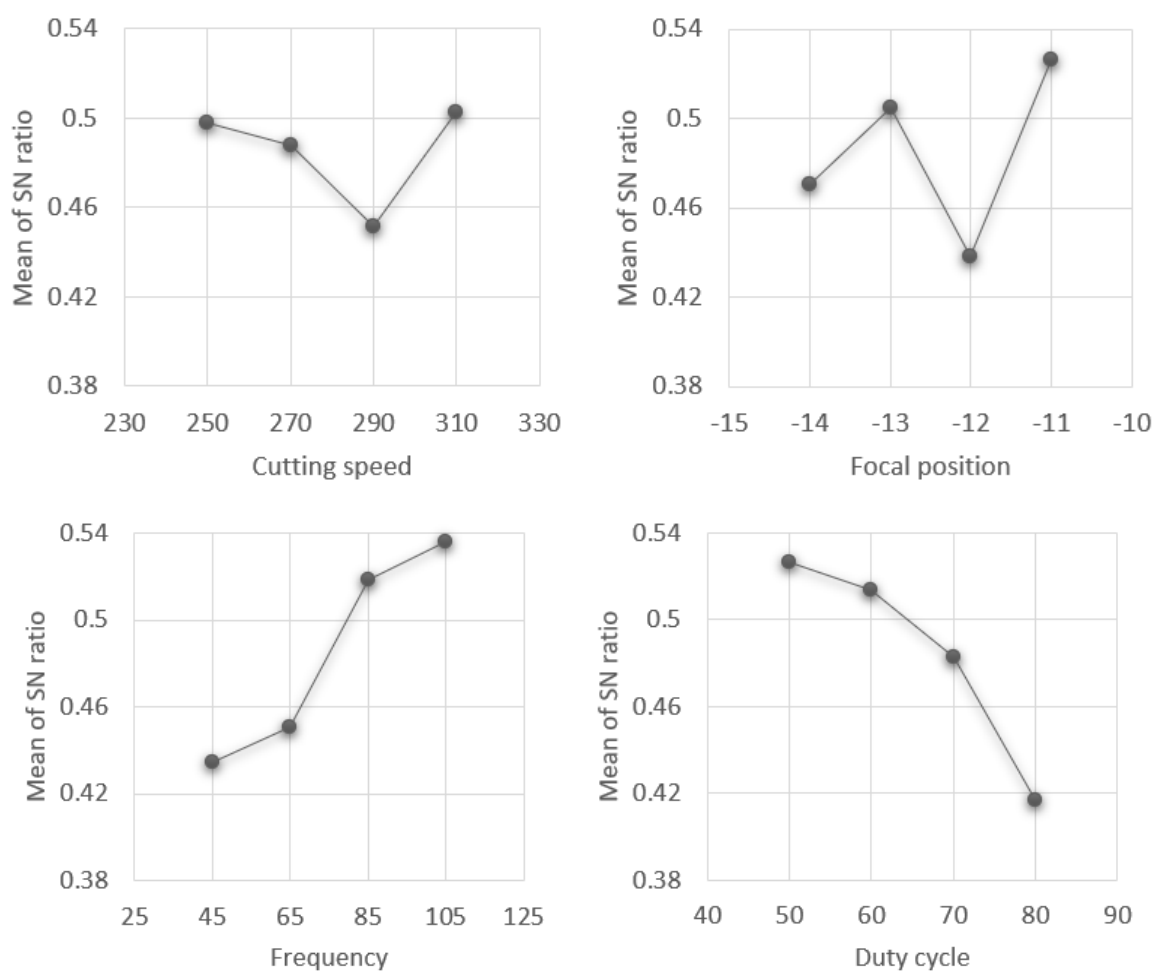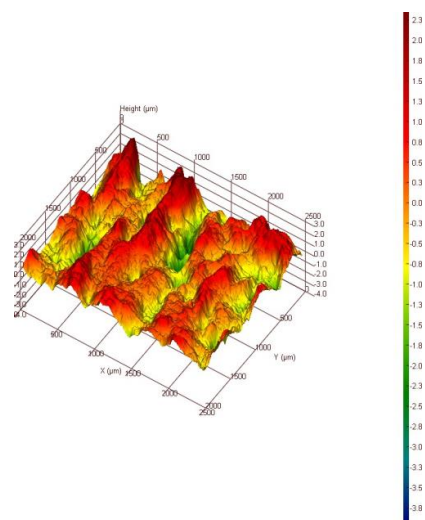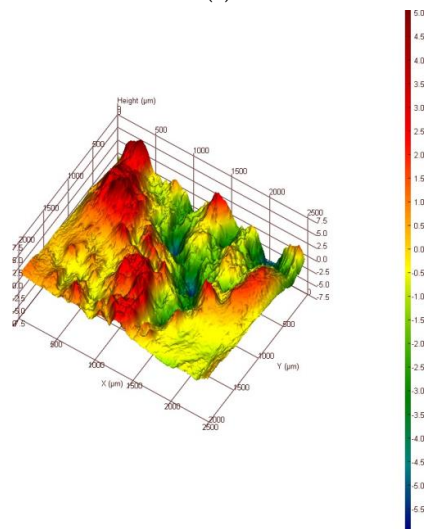
Figure 3. Grey relational grade graph of factors.

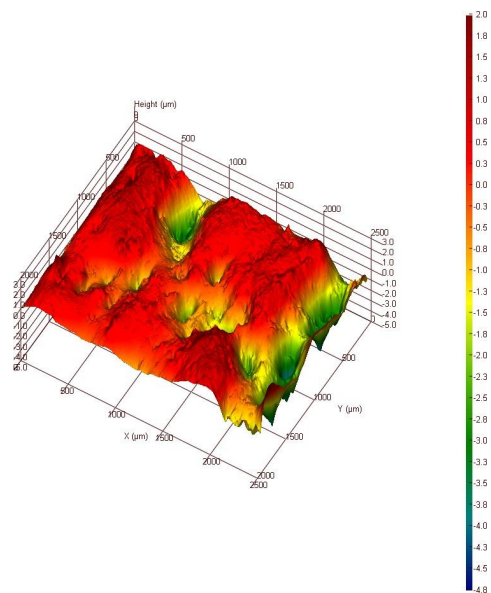**Table 6.** Grey Relational Grade (GRG) results by ANOVA.

| Parameters	DOF	Adj SS	Adj MS	F-Value	*p*-Value	Contr. (%)
CS	3	0.00651	0.00217	0.08	0.965	4.05
FP	3	0.01781	0.00593	0.23	0.872	11.08
F	3	0.02983	0.00994	0.38	0.775	18.55
DC	3	0.02861	0.00953	0.37	0.784	17.79
Residual error	3	0.07802	0.026008			48.53
Total	15	0.16078				

(**a**)

(**b**)

(**c**)

Figure 4. Surface topographies: (**a**) Sample 13, (**b**) Sample 15, and (**c**) Sample 6.

The numerical values obtained from optical profilometer were used to define average surface roughness values. Measurements and tests were assessed according to ISO 25 and ISO 178 declaration standards [36]. Arithmetic mean height (S_a) represents the absolute height from the mean plane. S_a is calculated according to Equation (6). [37]. "*A*" represents Unit Area, "*Z*" represents Height, and "*x*" and "*y*" represent the measurement coordinates.

$$S_a = \frac{1}{A} \iint_A |Z(x,y)| \, dx \, dy \tag{6}$$

When the results obtained were examined, the *Sa* value of the sample with the highest GRG value was also the lowest, which was 0.531 µm. When the surface topography was examined, a smoother topography was obtained compared to the other samples. The *Sa* value of the sample with the average GRG value was measured as 0.622 µm. The *Sa* value of the sample with the lowest GRG value was determined as 0.961 µm. The red color intensity in the surface topography of the sample with the average GRG value is due to the measurement scale. As an example of the cut samples, the surface images of the samples with the highest, lowest, and average GRG values are given in Figure 5.

(**a**)   (**b**)   (**c**)
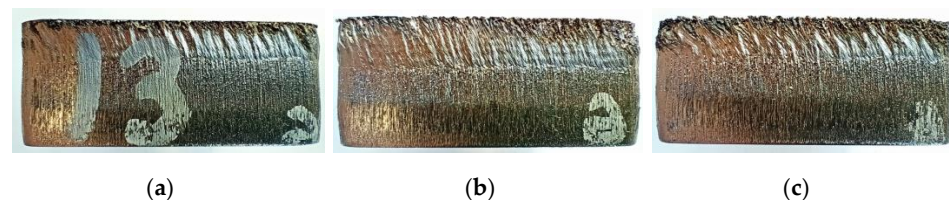
Figure 5. Surface views: (**a**) Sample 13, (**b**) Sample 15, and (**c**) Sample 6.

4. Conclusions

The aim of this present research was to establish the optimum process parameters (cutting speed, focal position, frequency and duty cycle) in cutting 20 mm-thick AISI304L (DIN EN 1.4301) quality stainless-steel material on a fiber laser bench. Within the scope of this study, experiments were performed according to the experimental table created using Taguchi experimental design method, and the surface roughness values and kerf widths were measured. With the help of the Taguchi method, the optimal parameter combination results obtained for the minimum surface roughness (SR) and minimum kerf width (KW) were $CS_4FP_1F_4DC_1$ and $CS_1FP_3F_3DC_3$, respectively. Additionally, according to results achieved by ANOVA, the order of importance for surface roughness was DC > CS > FP > F; for KW, it was listed as F > CS > FP > DC.

Furthermore, considering both the surface roughness and kerf width, the values of contribution ratios on the multiple response functions and optimum cutting process parameter level combinations were achieved by the GRA method. When all cases are examined, Experiment 13 ($CS_4FP_1F_4DC_1$) demonstrates the maximum multiple performance characteristics. The highest GRG value was shown with this combination; moreover, the surface roughness (SR) and kerf width (KW) values were detected as 8.31 µm and 0.33 mm, respectively.

The ANOVA method of analysis was applied to calculate the participation of every parameter on multiple responses. The parameter of frequency (F) is the most important variable on the multiple responses, with an effect of 18.55%. The duty cycle (DC) and focal position (FP) were the second and third most effective parameters, respectively. Additionally, according to results achieved by ANOVA, the most effective process parameter on kerf width was frequency, with the ratio of 31.2%. Duty cycle was found to be the most effective parameter on surface roughness, with an effect ratio of 49.01%. Furthermore, the Sa values of the samples with the highest, average, and lowest GRG values were 0.531 µm, 0.622 µm, and 0.961 µm, respectively. It has been determined that the optimum parameters for minimum surface roughness and minimum kerf width for fiber laser cutting of 20 mm-thick AISI 304L (DIN EN 1.4301) material were 310 mm/min for cutting speed, −11 mm for focal position, 105 Hz for frequency, and 60% for duty cycle.

Further Research Recommendations

In order to observe the effects of parameters' interactions (cutting speed × focal position, cutting speed × frequency, cutting speed × duty cycle, frequency × duty cycle, focal position × duty cycle, focal position × frequency), the effects can be evaluated in several different experiments with changing values by extra thicker and thinner samples. Further studies of these samples might provide other useful information regarding cutting with different parameters.

Author Contributions: Conceptualization, M.A and Y.A.T.; methodology, Y.A.T.; validation, C.Y., M.A. and Y.A.T.; investigation, M.A.; resources, A.T. and Ö.A.; writing—original draft preparation, Y.A.T. and M.A.; writing—review and editing, C.Y. and M.A.; supervision, N.Y. and C.Y. All authors have read and agreed to the published version of the manuscript.

Data Availability Statement: Datasets related to these studies, findings, and results as reported are included in the manuscript itself.

Conflicts of Interest: The authors declare no conflict of interest.

References

1. Shamlooei, M.; Zanon, G.; Valli, A.; Bison, P.; Bursi, O.S. Investigation of thermal behaviour of structural steel S235N under laser cutting process: Experimental, analytical, and numerical studies. *Eng. Struct.* **2022**, *269*, 114754. [CrossRef]
2. Liu, Y.; Zhang, S.; Zhao, Y.; Ren, Z. Experiments on the kerf quality characteristic of mild steel while cutting with a high-power fiber laser. *Opt. Laser. Technol.* **2022**, *154*, 108332. [CrossRef]
3. Ullah, S.; Li, X.; Guo, G.; Rodríguez, A.R.; Li, D.; Du, J.; Cui, L.; Wei, L. Energy efficiency and cut-quality improvement during fiber laser cutting of aluminum alloy in the different hardened conditions. *Mater. Today Commun.* **2022**, *33*, 104236. [CrossRef]
4. Lopez, A.B.; Assunção, E.; Quintino, L.; Blackburn, J.; Khan, A. High-power fiber laser cutting parameter optimization for nuclear Decommissioning. *Nucl. Eng. Technol.* **2017**, *49*, 865–872. [CrossRef]
5. Tamura, K.; Ishigami, R.; Yamagishi, R. Laser cutting of thick steel plates and simulated steel components using a 30 kW fiber laser. *J. Nucl. Sci. Technol.* **2016**, *53*, 916–920. [CrossRef]
6. Wandera, C.; Kujanpää, V. Optimization of parameters for fiber laser cutting of a 10 mm stainless steel plate. *Proc. Inst. Mech. Eng. Part B J. Eng. Manuf.* **2011**, *225*, 641–649. [CrossRef]
7. Wandera, C.; Kujanpää, V.; Salminen, A. Laser power requirement for cutting thick-section steel and effects of processing parameters on mild steel cut quality. *Proc. Inst. Mech. Eng. Part B J. Eng. Manuf.* **2011**, *225*, 651–661. [CrossRef]
8. Scintilla, L.D.; Tricarico, L.; Wetzig, A.; Beyer, E. Investigation on disk and CO_2 laser beam fusion cutting differences based on power balance equation. *Int. J. Mach. Tools Manuf.* **2013**, *69*, 30–37. [CrossRef]
9. Arteaga, F. CO_2 vs. Fiber Laser Technology: Which Is Right for You? 2022. Available online: https://bystronic.com/usa/en-us/news/130204-co2-vs-fiber-laser (accessed on 29 November 2022).
10. Powell, J.; Kaplan, F.H. A technical and commercial comparison of fiber laser and CO_2 laser cutting. *ICALEO* **2021**, *2012*, 277–281. [CrossRef]
11. Patel, A.; Bhavsar, S.N. Experimental investigation to optimize laser cutting process parameters for difficult to cut die alloy steel using response surface methodology. *Mater. Today Proc.* **2020**, *43*, 28–35. [CrossRef]
12. Amaral, I.; Silva, F.J.G.; Pinto, G.F.L.; Campilho, R.D.S.G.; Gouveia, R.M. Improving the cut surface quality by optimizing parameters in the fiber laser cutting process. *Procedia Manuf.* **2019**, *38*, 1111–1120. [CrossRef]
13. Ding, H.; Wang, Z.; Guo, Y. Multi-objective optimization of fiber laser cutting based on generalized regression neural network and non-dominated sorting genetic algorithm. *Infrared Phys. Technol.* **2020**, *108*, 103337. [CrossRef]
14. Magdum, V.B.; Kittur, J.K.; Kulkarni, S.C. Surface roughness optimization in laser machining of stainless steel 304 using response surface methodology. *Mater. Today Proc.* **2022**, *59*, 540–546. [CrossRef]
15. Kotadiya, D.J.; Pandya, D.H. Parametric Analysis of Laser Machining with Response Surface Method on SS-304. *Procedia Technol.* **2016**, *23*, 376–382. [CrossRef]
16. Anković, P.; Madić, M.; Radovanović, M.; Petković, D.; Mladenović, S. Optimization of Surface Roughness from Different Aspects in High-Power CO_2 Laser Cutting of AA5754 Aluminum Alloy. *Arab. J. Sci. Eng.* **2019**, *44*, 10245–10256. [CrossRef]
17. Rana, R.S.; Chouksey, R.; Dhakad, K.K.; Paliwal, D. Optimization of process parameter of Laser beam machining of high strength steels: A review. *Mater. Today Proc.* **2018**, *5*, 19191–19199. [CrossRef]
18. Kotadiya, D.J.; Kapopara, J.M.; Patel, A.R.; Dalwadi, C.G.; Pandya, D.H. Parametric analysis of process parameter for Laser cutting process on SS-304. *Mater. Today Proc.* **2018**, *5*, 5384–5390. [CrossRef]
19. Stelzer, S.; Mahrle, A.; Wetzig, A.; Beyer, E. Experimental investigations on fusion cutting stainless steel with fiber and CO_2 laser beams. *Phys. Procedia* **2013**, *41*, 399–404. [CrossRef]

20. Fomin, V.M.; Golyshev, A.A.; Malikov, A.G.; Orishich, A.M.; Shulyat'ev, V.B. Mechanical characteristics of high-quality laser cutting of steel by fiber and CO_2 lasers. *J. Appl. Mech. Tech. Phys.* **2015**, *56*, 726–735. [CrossRef]
21. Li, M. Evaluation of the effect of process parameters on the cut quality in fiber laser cutting of duplex stainless steel using response surface method (RSM). *Infrared Phys. Technol.* **2021**, *118*, 103896. [CrossRef]
22. Jadhav, A.; Kumar, S. Laser cutting of AISI 304 material: An experimental investigation on surface roughness. *Adv. Mater. Process. Technol.* **2019**, *5*, 429–437. [CrossRef]
23. Ghany, K.A.; Newishy, M. Cutting of 1.2 mm thick austenitic stainless steel sheet using pulsed and CW Nd:YAG laser. *J. Mater. Process. Technol.* **2005**, *168*, 438–447. [CrossRef]
24. Buj-Corral, I.; Costa-Herrero, L.; Domínguez-Fernández, A. Effect of process parameters on the quality of laser-cut stainless steel thin plates. *Metals* **2021**, *11*, 1224. [CrossRef]
25. Rajesh, K.; Murali Krishnam Raju, V.V.; Rajesh, S.; Sudheer Kumar Varma, N. Effect of process parameters on machinability characteristics of CO_2 laser process used for cutting SS-304 stainless steels. *Mater. Today Proc.* **2019**, *18*, 2065–2072. [CrossRef]
26. Aperam Inox America do Sul, S.A. *EN 10204 3.1 Quality Certificate*; Aperam Inox America do Sul S.A.: Belo Horizonte, Brazil, 2004.
27. Yuce, C. Multi-objective optimisation for indentation rate, nugget diameter and tensile load in resistance spot welding using Taguchi-based grey relational analysis. *Int. J. Mater. Prod. Technol.* **2021**, *63*, 321–338. [CrossRef]
28. Tutar, M.; Aydin, H.; Yuce, C.; Yavuz, N.; Bayram, A. The optimisation of process parameters for friction stir spot-welded AA3003-H12 aluminium alloy using a Taguchi orthogonal array. *Mater. Des.* **2014**, *63*, 789–797. [CrossRef]
29. Yuce, C.; Tutar, M.; Karpat, F.; Yavuz, N. The optimization of process parameters and microstructural characterization of fiber laser welded dissimilar HSLA and MART steel joints. *Metals* **2016**, *6*, 245. [CrossRef]
30. Caydas, U.; Hascalik, A. Use of the grey relational analysis to determine optimum laser cutting parameters with multi-performance characteristics. *Opt. Laser Technol.* **2008**, *40*, 987–994. [CrossRef]
31. Chen, M.F.; Sen Ho, Y.; Hsiao, W.T.; Wu, T.H.; Tseng, S.F.; Huang, K.C. Optimized laser cutting on light guide plates using grey relational analysis. *Opt. Lasers Eng.* **2011**, *49*, 222–228. [CrossRef]
32. Senthilkumar, V.; Adinarayanan, A.; Jagatheesan, K. Grey Relational Analysis (GRA) for optimization of CO_2 laser cutting of stainless steel. *Mater. Today Proc.* 2022, *in press*. [CrossRef]
33. Karthikeyan, R.; Senthilkumar, V.; Thilak, M.; Nagadeepan, A. Application of grey relational analysis for optimization of kerf quality during CO_2 laser cutting of mild steel. *Mater. Today Proc.* **2018**, *5*, 19209–19215. [CrossRef]
34. Pattanaik, A.K.; Panda, S.N.; Pal, K.; Mishra, D. A comparative investigation to process parameter optimization for spot welding using Taguchi based grey relational analysis and metaheuristics. *Mater. Today Proc.* **2018**, *5*, 11408–11414. [CrossRef]
35. Wan, X.; Wang, Y.; Zhao, D. Multiple quality characteristics prediction and parameter optimization in small-scale resistance spot welding. *Arab. J. Sci. Eng.* **2016**, *41*, 2011–2021. [CrossRef]
36. *ISO 25178-2*; Geometrical Product Specifications (GPS)—Surface Texture: Areal—Part 2: Terms, Definitions and Surface Texture Parameters. International Organization for Standardization: Geneva, Switzerland, 2012.
37. Cavusoglu, O. The 3D surface morphological investigation of laser cutting process of 2024-T3 aluminum alloy sheet. *Optik* **2021**, *238*, 166739. [CrossRef]